Article

Not peer-reviewed version

Multitarget Strategy for Treatment of Pulmonary Arterial Hypertension: Combination of Mesenchymal Cells with Novel PDE-4 Inhibitor

Bruno Eduardo Dematté , Juliana Ferreira Vasques , Almir Jordão da Silva-Junior , Lucas Silva Franco , Rodolfo do Couto Maia , Pedro De Sena Murteira Pinheiro , Rosalia Mendez-Otero , Tadeu Lima Montagnoli , Gisele Zapata-Sudo *

Posted Date: 2 December 2025

doi: 10.20944/preprints202512.0045.v1

Keywords: pulmonary arterial hypertension; right ventricle failure; cell therapy; PDE inhibition

Article

Multitarget Strategy for Treatment of Pulmonary Arterial Hypertension: Combination of Mesenchymal Cells with Novel PDE-4 Inhibitor

Bruno E. Dematté [1], Juliana Ferreira Vasques [2], Almir Jordão da Silva-Junior [3], Lucas Silva Franco [4], Rodolfo do Couto Maia [4], Pedro de Sena Murteira Pinheiro [4], Rosália Mendez-Otero [3], Tadeu Lima Montagnoli [5] and Gisele Zapata-Sudo [1,*]

[1] Programa de Pós-Graduação em Cardiologia, Instituto do Coração Edson Saad, Universidade Federal do Rio de Janeiro, Rio de Janeiro, RJ 21941-913, Brazil

[2] Instituto de Ciências Biomédicas, Universidade Federal do Rio de Janeiro, Rio de Janeiro, RJ 21941-902, Brazil

[3] Instituto de Biofísica Carlos Chagas Filho, Universidade Federal do Rio de Janeiro, Rio de Janeiro, RJ 21941-902, Brazil

[4] Laboratório de Avaliação e Síntese de Substâncias Bioativas, Instituto de Ciências Biomédicas, Universidade Federal do Rio de Janeiro, Rio de Janeiro, RJ 21941-902, Brazil

[5] Instituto de Química, Universidade Federal do Rio de Janeiro, Rio de Janeiro, RJ 21941-902, Brazil

* Correspondence: gsudo@icb.ufrj.br or gzsudo@gmail.com; Tel./Fax: +55-21-39386505

Abstract

Background/Objectives. Pulmonary arterial hypertension (PAH) is a rare but severe disease which leads to right ventricular (RV) maladaptation, failure and death. Currently approved drugs have limited impact on disease progression. A multitarget strategy consisted of activation of adenosine A_2B receptor and inhibition of phosphodiesterase-4 (PDE4) in combination with human mesenchymal stromal cells (hMSCs) was tested in PAH animal model. The main objective was to determine whether the combination improves pulmonary hemodynamics, vascular remodeling, and RV function, given the limited disease-modifying effects of approved vasodilators. **Methods.** Vascular reactivity was assessed in isolated rat pulmonary artery rings exposed to the dual target compound named LASSBio-1860 alone or in the presence of either A_2A (ZM-241385) or A_2B (MRS-1706) antagonist. PAH was induced in male Wistar rats through the administration of monocrothaline (MCT, 60 $mg \cdot kg^{-1}$). After confirmation of PAH, by the decrease of the ratio of pulmonary artery acceleration time and ejection time ratio (PAAT/TET), animals were randomized divided to receive vehicle, hMSC (single i.v. dose, 1×10^5 cells), LASSBio-1860 (62 $mg \cdot kg^{-1} \cdot day^{-1}$, p.o., 14 days), or the combination. Outcomes included PAAT/TET and RV cardiac output (RV-CO) using echocardiography, RV systolic pressure (RVSP) by direct puncture, Fulton index and RV wall thickness, lung histology (perivascular cell counts and wall thickness), and RV protein expression (TGF-β, CaMKII) by Western blot. **Results**. LASSBio-1860 produced endothelium-independent vasorelaxation of rat pulmonary arteries, consistent with A_2B agonism and PDE4 inhibition responses. In MCT-induced PAH, the combination of LASSBio-1860 with hMSCs promoted: 1. Recovery of PAAT/TET and RV-CO; 2. Decrease of RVSP; 3. Reduction of RV hypertrophy, vascular inflammation and remodeling; 4. Downregulation of ventricular TGF-β and CaMKII. **Conclusions**. Combination of LASSBio-1860 with hMSC improved RV function, attenuated pulmonary hypertension, RV and vascular remodeling; reduced inflammatory/proliferative signaling in MCT induced-PAH, supporting a promising multitarget therapeutic strategy for PAH.

Keywords: pulmonary arterial hypertension; right ventricle failure; cell therapy; PDE inhibition

 doi:10.20944/preprints202512.0045.v1

1. Introduction

Pulmonary arterial hypertension (PAH) is a rare and progressive disorder, characterized by pulmonary vessels remodeling and hypertrophy. This maladaptive remodeling leads to luminal narrowing of small pulmonary arteries, causing elevated pulmonary vascular resistance and right ventricular afterload, ultimately leading to right heart failure and death [1]. PAH is classified as a precapillary hypertension, with normal pulmonary capillary wedge pressure and pulmonary arterial pressure (mPAP) greater than 20 mmHg at rest [2]. Among the several pharmacological alternatives, the current treatment of PAH addresses vascular relaxation, focusing only in hemodynamic aspects and not considering the mechanisms involved in disease progression. Consequently, PAH prognosis remains poor, with mortality rates approximately 50% within seven years despite treatment [3].

Although five drug classes are approved for clinical use – endothelin receptor antagonists, phosphodiesterase-5 inhibitors, prostacyclin analogues, guanylate cyclase stimulators, and calcium channel blockers – the monotherapy is frequently limited by significant adverse effects besides modest efficacy [4]. Endothelin receptor antagonists are associated with hepatotoxicity and peripheral edema [5]; prostacyclin analogues often cause systemic hypotension [6]; and phosphodiesterase-5 inhibitors can cause headaches and visual disturbances [7]. Those adverse events affect treatment adherence and quality of life of patients [8]. Vasodilator-based approved drugs fail to interfere with the critical aspects of PAH progression, such as endothelial-to-mesenchymal transition (EndMT) [15], inflammation and fibrosis [16,17].

An alternative to improve these conditions was attempted with the design and synthesis of a novel compound named LASSBio-1860, which has a dual profile, inhibition of phosphodiesterase-4 (PDE4) and activation of adenosine A_2 receptors [18,19]. LASSBio-1860 represents a potential dual-mechanism therapy for PAH within a multitarget strategy to modify disease progression. The simultaneous interference in proliferative and inflammatory pathways, LASSBio-1860 could be considered a potential modulator of PAH pathogenesis.

To further enhance therapeutic efficacy, the combination of LASSBio-1860 with human mesenchymal stem cells (hMSC) may offer synergistic benefits by integrating pharmacological and cell-based approaches to attenuate vascular remodeling while conferring cardioprotection [27]. The present work investigated the effects of LASSBio-1860 in combination with hMSC in a monocrotaline(MCT)-induced model of PAH in rats, including the hemodynamic, morphometric, and molecular parameters relevant to disease progression.

2. Results

2.1. Dual Target of LASSBio-1860

The vasodilatory effect of LASSBio-1860 was initially assessed in isolated pulmonary artery rings, both with and without endothelium. LASSBio-1860-induced relaxation of pulmonary artery was not altered by the mechanical removal of endothelium, suggesting that its action is independent of the functional endothelial cells. As shown in Figure 1, LASSBio-1860 induced a concentration-dependent pulmonary artery rings relaxation, with an EC_{50} of 2.80 ± 0.29 μM. The presence of ZM-241385 (300 nM), a selective A_2A receptor antagonist, did not change the potency of LASSBio-1860 (EC_{50} = 2.80 ± 0.35 μM), indicating that A_2A subtype receptor is not involved in the vasodilatory effect. In contrast, exposure to MRS-1706 (100 nM), an adenosine A_2B receptor antagonist, promoted a rightward shift of the concentration–response curve, resulting in a significantly higher EC_{50} (5.55 ± 0.78 μM, $p < 0.05$).

 doi:10.20944/preprints202512.0045.v1

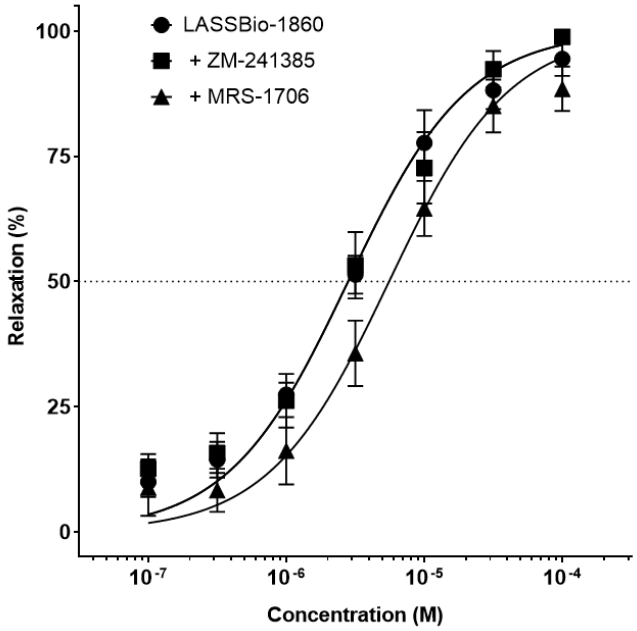

Figure 1. Relaxation of pulmonary artery rings without endothelium induced by LASSBio-1860. Tissues were incubated with vehicle (n = 5), ZM-241385 (300 nM; n = 7), or MRS1706 (100 nM; n = 6). LASSBio-1860 promoted concentration-dependent relaxation with EC_{50} of 2.80 ± 0.29 μM, similarly with EC_{50} of 2.80 ± 0.35 μM in the presence of ZM-241385 (A_2A antagonist). MRS-1706, an A_2B antagonist, increased the EC_{50} to 5.55 ± 0.78 μM ($p < 0.05$). Data were expressed as mean ± SEM.

These findings suggest a predominant contribution of adenosine A_2B receptor activation to the vasodilatory effect response induced by LASSBio-1860 in pulmonary arteries over adenosine A_2A receptors.

To further assess the role of PDE inhibition and the activation of cAMP/PKA axis for the vasodilatory effect of LASSBio-1860, pulmonary artery rings were exposed to the β-adrenergic agonist, isoproterenol (Figure 2a). LASSBio-1860 preincubation produced a leftward shift of the isoproterenol concentration-relaxation curve, with decrease of EC_{50} from 56.17 ± 7.46 to 33.17 ± 2.79 nM. Also, an increase of the maximal relaxation induced by isoproterenol was increased in the presence of LASSBio-1860 (Figure 2b).

β-adrenergic agonists such as isoproterenol relax the vessel by activating adenylyl cyclase (AC) and increasing intracellular cAMP which breakdown could be limited by inhibition of PDE4, leading to an increased relaxation of pulmonary arteries. Elevation of cAMP, either by stimulating its synthesis or by reducing its degradation, is an efficient strategy to enhance pulmonary vasodilation.

 doi:10.20944/preprints202512.0045.v1

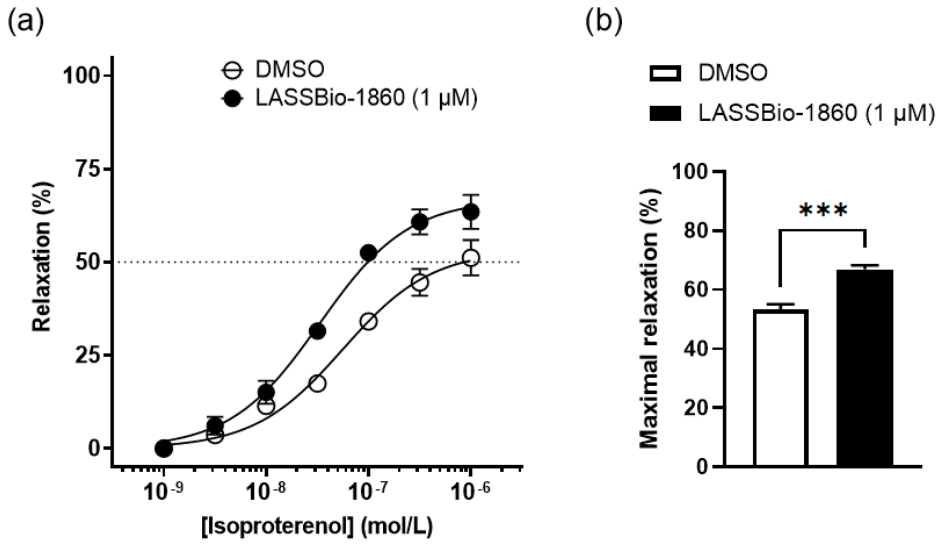

Figure 2. Relaxation of pulmonary artery rings induced by isoproterenol. **(a)** Rings were incubated with vehicle (n = 5) or LASSBio-1860 (1 μM; n = 5) and cumulatively exposed to isoproterenol. Isoproterenol promoted concentration-dependent relaxation with EC_{50} of 56.17 ± 7.46 nM (vehicle) and 33.17 ± 2.79 nM (LASSBio-1860), indicating enhanced β-adrenergic vasorelaxation in the presence of LASSBio-1860. **(b)** Maximal relaxation (%) DMSO vs. LASSBio-1860. Bars show mean ± SEM (n = 5/group); ***p < 0.001 vs. vehicle (unpaired two-tailed t-test). Data were expressed as mean ± SEM.

2.2. Combination of LASSBio-1860 with Mesenchymal Cells

After 14 days of PAH induction, PAAT/TET declined from 0.41 ± 0.06 to 0.27 ± 0.01, as shown in Figure 3. At the end of protocol, isolated therapies produced only modest increase of PAAT/TET, 0.27 ± 0.01 and 0.28 ± 0.01 for hMSC (10^5 cells) and LASSBio-1860 (62 mg/kg), respectively. The combination of hMSC + LASSBio-1860 elevated PAAT/TET to 0.31 ± 0.06 higher than the 0.26 ± 0.01 observed on untreated PAH ($p < 0.05$).

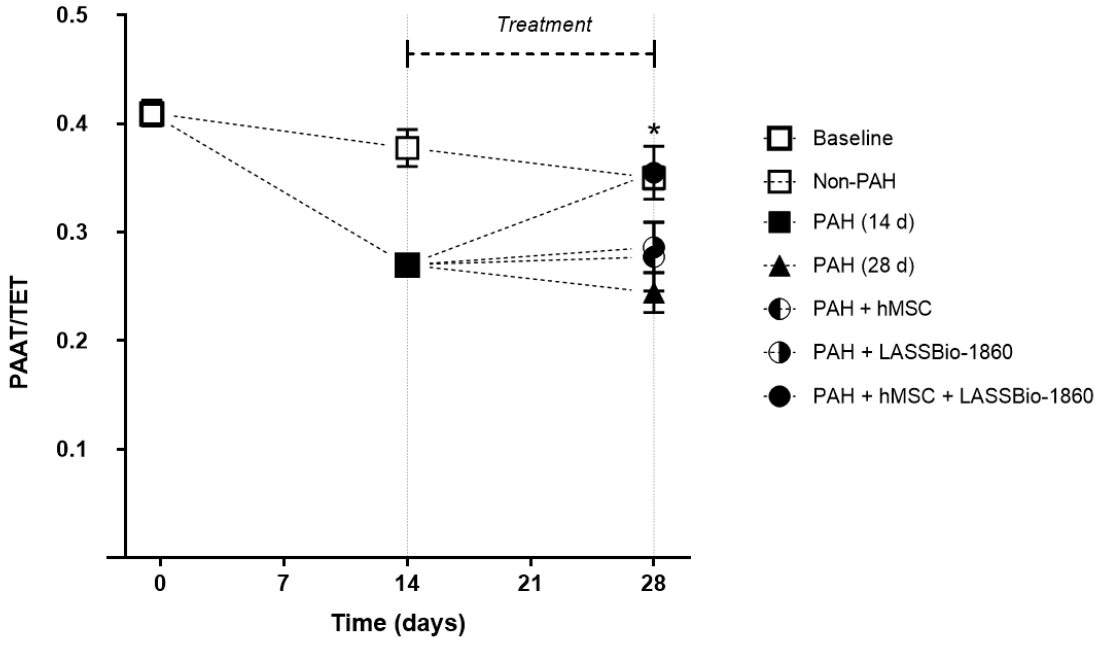

 doi:10.20944/preprints202512.0045.v1

Figure 3. Echocardiographic assessment of PAAT/TET across disease progression and treatment. The pulmonary artery acceleration time/ejection time ratio (PAAT/TET) was measured by pulsed-wave Doppler at baseline (day 0), after PAH establishment (day 14), and following a 14-day treatment period (day 28). From day 14 to 28, animals received: vehicle (PAH), hMSC (single administration, 1×10^5 cells), LASSBio-1860 (62 mg·kg^{-1}·day^{-1}, p.o.), or the association (same dose and cell amount). Mean ± SEM values were: baseline, 0.409 ± 0.060; PAH (14 d), 0.269 ± 0.010; PAH (28 d), 0.257 ± 0.010; PAH + hMSC, 0.273 ± 0.010; PAH + LASSBio-1860, 0.277 ± 0.010; PAH + hMSC + LASSBio-1860, 0.355 ± 0.025. PAH reduced PAAT/TET from baseline to day 14. Association therapy increased PAAT/TET versus untreated PAH (*$p < 0.05$ vs. PAH, 28 d; n = 5-7).

As presented in Figure 4a, PAH induction resulted in an increase on the right ventricular systolic pressure (RVSP) from 19.21 ± 4.15 (control group) to 71.03 ± 11.53 mmHg. Either hMSC or LASSBio-1860 reduced RVSP to 45.09 ± 6.22 mmHg and 46.94 ± 4.30 mmHg. Combined therapy of hMSC and LASSBio-1860 significantly reduced RVSP to 37.58 ± 3.27 mmHg. Figure 4b shows right ventricular cardiac output (RV-CO), assessed by echocardiography. PAH group exhibited marked decreased RV-CO of 65.2 ± 5.2 mL·min^{-1} compared to the Non-PAH group, 91.3 ± 9.7 mL·min^{-1}, indicating disease-induced cardiac dysfunction. Recovery of this parameter to 102.4 ± 5.9 mL·min^{-1} was observed after treatment with the combination of hMSC + LASSBio-1860. Administration of LASSBio-1860 or hMSC alone restored RV-CO to levels near those of the control group 98.1 ± 11.9 and 89.8 ± 10.9 mL·min^{-1}.

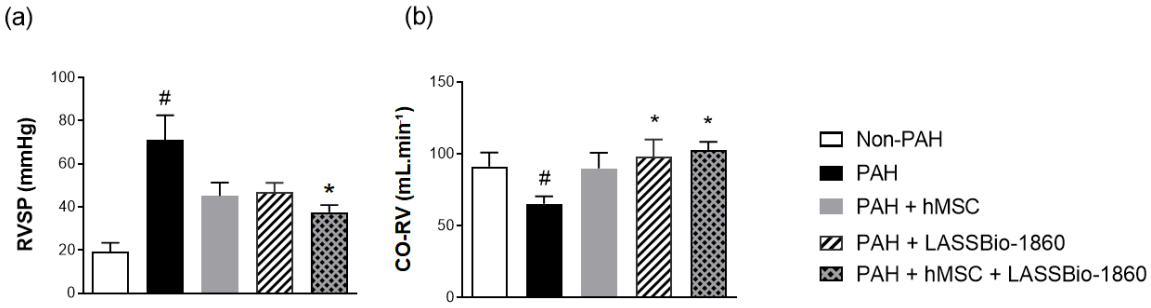

Figure 4. Effects of LASSBio-1860 and hMSC therapy on right-ventricular hemodynamics in PAH. (a) Right ventricular systolic pressure (RVSP, in mmHg) measured via right ventricular puncture (mean ± SEM): Non-PAH, 19.21 ± 4.15; PAH, 71.03 ± 11.53; PAH + hMSC, 45.09 ± 6.22; PAH + LASSBio-1860, 46.94 ± 4.30; PAH + hMSC + LASSBio-1860, 37.58 ± 3.27; and (b) Right ventricular cardiac output (CO-RV, mL·min^{-1}) was measured echocardiographically at the conclusion of the protocol: Non-PAH, 91.27 ± 9.67; PAH, 65.22 ± 5.19; PAH + hMSC, 89.82 ± 10.94; PAH + LASSBio-1860, 98.11 ± 11.89; PAH + hMSC + LASSBio-1860, 102.40 ± 5.98 (# $p < 0.05$ vs. Non-PAH; * $p < 0.05$ vs. PAH).

In addition to right-ventricular functional evaluation, structural parameters were also investigated. MCT produced marked RV remodeling and hypertrophy relative to Non-PAH, increasing the Fulton index from 28.3 ± 1.0 to 55.8 ± 3.3 and RV anterior wall thickness from 0.65 ± 0.07 to 1.02 ± 0.07 mm (Figure 5). In contrast, the combined regimen (hMSC + LASSBio-1860) significantly reduced both indices compared with PAH (Fulton 33.8 ± 2.6%; RV thickness 0.68 ± 0.04 mm; $P < 0.05$). These data indicate that concomitant cell therapy and LASSBio-1860 treatment was more effective in RV hypertrophic/fibrotic remodeling reduction than either administration alone.

 doi:10.20944/preprints202512.0045.v1

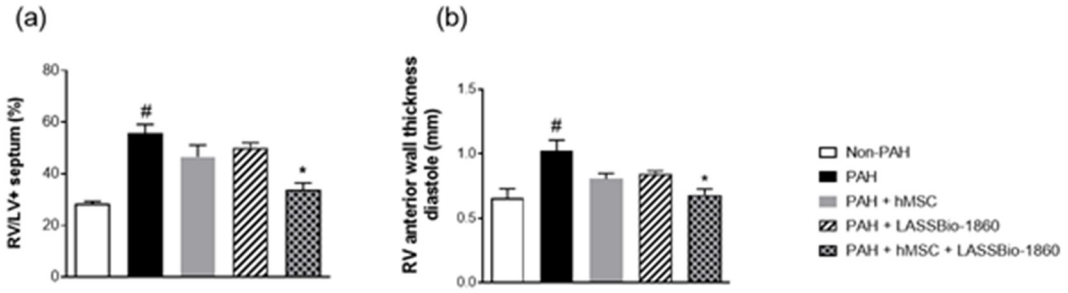

Figure 5. Right-ventricular remodeling in monocrotaline-induced PAH and after treatments.(a) Fulton index (RV/[LV+septum], %). (b) Right-ventricular (RV) anterior wall thickness in diastole (mm) was measured echocardiographically. Bars show mean ± SEM. One-way ANOVA with Tukey's post-hoc test. # $P < 0.05$ vs. Non-PAH; * $P < 0.05$ vs. PAH.

Histopathological analysis (Figure 6) corroborated the anti-remodeling effect of the combined regimen. Hematoxylin–eosin lung sections from PAH animals exhibited a dense perivascular inflammatory infiltrate and medial hypertrophy relative to Non-PAH. In contrast, the combined therapy (hMSC + LASSBio-1860) significantly attenuated inflammatory infiltration and reduced wall thickness compared with untreated PAH. These findings indicate that the association strategy mitigates both the inflammatory and structural components of pulmonary vascular remodeling in this model.

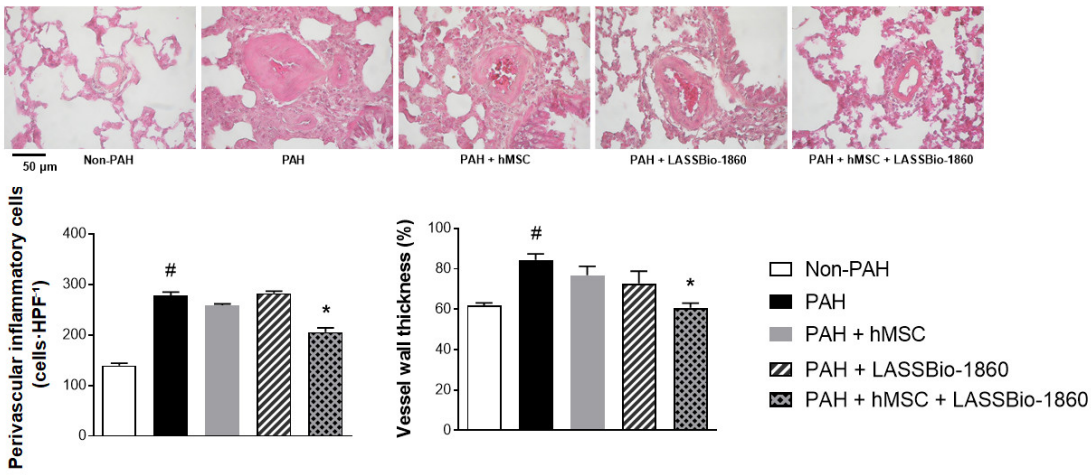

Figure 6. PAH-induced perivascular inflammation and vascular remodeling reduction in association group. H&E-stained lung section illustrating perivascular inflammatory tissue and medial thickening in PAH, with attenuation after association therapy. Perivascular inflammatory cells (cells·HPF^{-1}) counted at 400× within one vessel diameter of the external elastic lamina. PAH increased perivascular cell counts versus Non-PAH (#$P <$ 0.05); combined treatment significantly reduced infiltration compared with PAH (*$P < 0.05$). Bottom, right: Vessel wall thickness (% of vessel diameter). PAH increased wall thickness relative to Non-PAH (#$P < 0.05$). The combined therapy (hMSC + LASSBio-1860) markedly decreased wall thickness versus PAH (*$P < 0.05$). Bars show mean ± SEM; groups were compared by one-way ANOVA with post-hoc multiple comparisons.

In cardiac tissue, western blot normalized to GAPDH demonstrated that PAH markedly increased the expression of both transforming growth factor beta (TGF-β) and calcium/calmodulin-dependent protein kinase type II (CaMKII) relative to Non-PAH control. Neither hMSC monotherapy nor LASSBio-1860 alone reduced these elevations. In contrast, the combined treatment (hMSC + LASSBio-1860) produced a robust reduction of TGF-β and CaMKII, significantly lower than PAH (Figure 7). TGF-β leads to cardiac fibrosis and fibroblast activation under RV pressure overload and

 doi:10.20944/preprints202512.0045.v1

PAH, while CaMKII is a central integrator of pathological Ca^{2+} signaling in myocardium, promoting hypertrophy, inflammation, and adverse remodeling. These data indicate that, at the myocardial level, concomitant cell therapy and LASSBio-1860 more effectively counterregulate profibrotic (TGF-β), inflammatory and proliferative (CaMKII) signaling than either intervention alone.

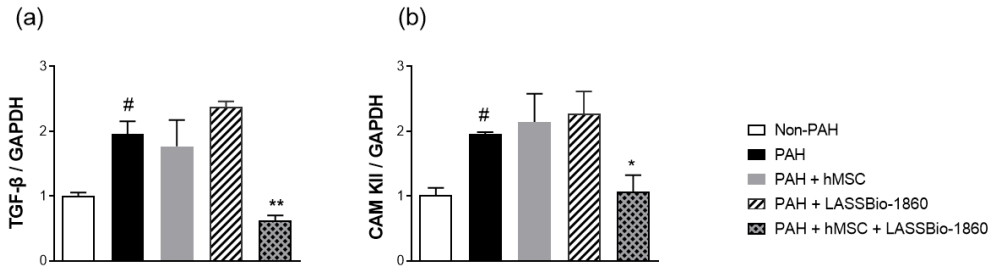

Figure 7. Association of LASSBio-1860 with hMSC reduces profibrotic and proliferative signaling in cardiac tissue. Quantification of Western blots in right ventricular myocardium (normalized to GAPDH) shows that PAH increases TGF-β and CaMKII expression versus Non-PAH controls (# $p<0.05$). Neither hMSC alone nor LASSBio-1860 alone attenuated these elevations. In contrast, the combined treatment (hMSC + LASSBio-1860) markedly reduced both TGF-β and CaMKII to levels significantly lower than PAH (* $p<0.05$; ** $p<0.01$ vs PAH). Bars represent mean ± SEM; n=3 per group.

3. Discussion

The pathogenesis of PAH is complex and multifactorial, including endothelial cell dysfunction [9], proliferation of pulmonary arterial smooth muscle cells (PASMCs) [10], adventitial fibroblast activation and inflammation, contributing to medial thickening, hypertrophy and vessels remodeling [11].

In the pulmonary vasculature, activation of G protein-coupled adenosine receptors A_2A and A_2B induces vasodilation through activation of adenylate cyclase, and increase of intracellular 3′,5′-cyclic adenosine monophosphate (cAMP) [20]. Adenosine receptor A_2B has been implicated in the reduction of vascular remodeling by reducing smooth muscle cell proliferation [21,22]. Moreover, PDE4 manages the hydrolysis of cAMP, and its inhibition leads to increased intracellular cAMP levels, thereby activating protein kinase A (PKA) and producing vasorelaxation of pulmonary arterial smooth muscle cells [23]. PDE4 inhibition has been shown to mitigate EndMT, a critical contributor to pulmonary vascular remodeling and disease progression, reinforcing its role as a therapeutic target in PAH [24]. PDE4 is also the dominant isoenzyme in inflammatory cells, which inhibition could attenuate transforming growth factor beta (TGF-β) signaling via cAMP/PKA activation in human lung fibroblasts, indicating broader antifibrotic and anti-inflammatory potential [25,26].

Emerging strategies have been proposed using hMSC due to their efficiency to modulate pulmonary vascular paracrine mediators [12]. Preclinical studies using MSCs and their extracellular vesicles demonstrated anti-inflammatory and antiproliferative effects on the pulmonary vasculature and a protective effect on RV [13]. Hence, MSCs represent a potential approach to address the multiple processes involved in PAH pathogenesis [14].

Our data suggest a new, multitarget disease-modifying approach for pulmonary arterial hypertension (PAH). LASSBio-1860 promoted an endothelium-independent relaxation in isolated pulmonary artery through the activation of A_2B adenosine receptor and inhibition of PDE4. The combination of LASSBio-1860 and hMSC reduced RVSP, restored RV-CO, lowered RV hypertrophy and attenuated perivascular tissue inflammation and medial pulmonary vessel thickeness. Additionally, the administration of the combination down-regulated TGF-β and CaMKII, important inflammatory, profibrotic and proliferative markers in animal model of PAH [28–31]. Our hypothesis is that the dual cAMP-elevating mechanisms related to activation of A_2B adenosine receptor and inhibition of PDE4 induced by LASSBio-1860 could increase the efficacy of the paracrine signaling of

 doi:10.20944/preprints202512.0045.v1

hMSC to improve pulmonary vascular remodeling and RV maladaptation. The combined regimen achieved greater improvement in hemodynamic and structural markers than either LASSBio-1860 or hMSCs alone, suggesting a synergistic effect on pulmonary vascular and right ventricular remodeling.

Our findings are in accordance with preclinical studies, in which the activation of A_2B adenosine receptor reduces PASMC growth [21]. Activation of the Gs-coupled A_2B adenosine receptor in the pulmonary artery leads to the amplification of cAMP/PKA signaling, which confers anti-mitogenic properties [20]. Interestingly, some studies report an increased expression of A_2B adenosine receptor in lungs of PAH patients [32,33]. Furthermore, some preclinical studies in different PAH models suggest that activation of the adenosine A_2B receptors on macrophages plays an active role in the pathogenesis of lung fibrosis and PH [34]. Moreover, PDE4 inhibition diminish cAMP hydrolysis and increases PKA-dependent vascular muscle relaxation [35]; regulates baseline sarcoplasmic reticulum Ca^{2+} release and cardiac contractility [36]; counterbalances proliferative/inflammatory mechanisms in PASMCs [37]; and downregulate the fibroblast-to-myofibroblast transition (FMT) and proliferative activity in lung fibroblasts [31]; as well as, particularly PDE4B, regulates EndMT [24] and vascular inflammation in the lungs.

Preclinical data demonstrate that MSCs and their extracellular vesicles (EV) [38] promote beneficial changes in pathophysiology in PAH [39], providing benefits beyond vasodilation [40]. MSC-based products prevent or reverse pulmonary vascular remodeling, improve hemodynamics and RV function, and reduce perivascular inflammation [41,42]. The reprograming of immune and vascular pathways, promote suppression of NF-κB through PDE inhibition and PKA phosphorylation; thereby limiting smooth-muscle proliferation [43]. These effects provide a biologic rationale for pairing hMSC-mediated paracrine immunomodulation altogether with pharmacological agents to interferer with remodeling. Positive results in clinical studies with umbilical cord MSC–derived products, in severe pediatric PAH, reinforces the translational development [44]. The combined action of LASSBio-1860 and the anti-inflammatory properties of cellular therapy [45] represents a novel approach to mitigate cardiac and pulmonary vascular remodeling, in addition to causing vascular relaxation.

Currently, approved PAH therapies primarily produce vasodilation and reduce RV pressure, but have limited impact on vascular remodeling and heart maladaptive processes. Recent clinical trials in PAH have provided growing support for targeting anti-inflammatory, antiproliferative, and antifibrotic pathways as novel therapeutic strategies [42,45,46]. Those indicate that targeting inflammatory and proliferative signaling pathways can improve patient outcomes. This strategy, consisted of a fusion protein that sequesters TGF-β and activins to favor BMP signaling induced by sotatercept, reduces vessel remodeling [47], which shows a promising successful intervention.

The limitation of this work is the use of a single rodent model and a fixed treatment regimen, along with a limited pathways evaluation, which may not fully capture the complex and multifaceted PAH pathophysiology. LASSBio-1860 is a new drug prototype and further studies are required to comprehensively evaluate its safety profile.

Finally, the combination of the increase of cAMP and hMSC-based therapy may contribute to disease modification in PAH. These findings indicate that the elevation of cAMP level, through activation of adenosine A_2B receptors and inhibition of PDE4 together with the paracrine immunomodulatory hMSC actions [46] could be a new strategy for interfering with the structural/inflammatory axes involved in PAH progression.

4. Materials and Methods

4.1. Drugs and Reagents

E)-N'-3,4-dimethoxybenzylidenebenzo[b]thiophene-2-carbohydrazide, named LASSBio-1860 (Figure 8), was synthetized at Laboratório de Avaliação e Síntese de Substâncias Bioativas , Universidade Federal do Rio de Janeiro, Brazil. Ketamine and isoflurane were provided by Cristália

 doi:10.20944/preprints202512.0045.v1

Produtos Químicos e Farmacêuticos Ltd.a (Itapira, SP, Brazil). Isoproterenol and monocrotaline were purchased from Sigma-Aldrich (St. Louis, MO, USA).

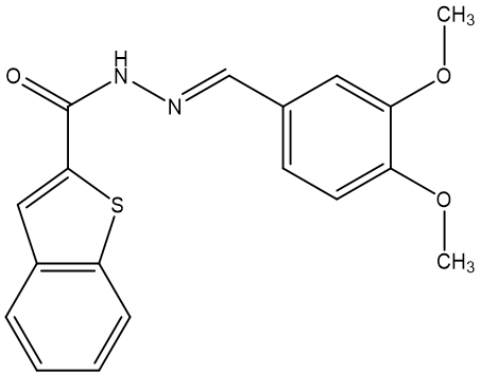

Figure 8. Chemical structure of LASSBio-1860, an N-acylhydrazone derivative reported to inhibit PDE4 catalytic activity by 70% and to exhibit sub-10 μM affinity at adenosine A2 receptors, supporting its candidacy as a dual-mechanism prototype for PAH therapy [19].

4.2. Animals and Experimental Design

All experimental protocols were approved by the Committee on Ethics in the Use of Animals at Universidade Federal do Rio de Janeiro (license number 018/23). Male Wistar rats (200-250 g) were kept under a light/dark cycle of 12 hours at 24 °C, with free access to water and pellet-type feed.

4.3. Vascular Reactivity of Pulmonary Artery Rings

Pulmonary arteries were carefully dissected from euthanized Wistar rats and placed in a physiological solution (composition in mM: NaCl 123, KCl 4.7, $CaCl_2$ 1.2, $MgSO_4$ 1.2, KH_2PO_4 1.2, $NaHCO_3$ 15.5 and glucose 11.1), pH 7.4, maintained at 37 °C, and oxygenated with 95% O_2/5% CO_2. Vessels were cleaned of connective tissue and rings (2–3 mm in length) were obtained with or without intact endothelium, confirmed by lack of acetylcholine-induced relaxation (10 μM) in precontracted aorta (with phenylephrine,10 μM). Rings were positioned in organ baths for isometric tension recording using force transducers connected to Lab Chart software (Version 7.0, ADInstruments, Inc., Sydney, Australia). After 60 min under a resting tension of 1.5 g, rings were exposed to cumulative concentrations of LASSBio-1860 (10^{-7} to 10^{-4} M) to obtain concentration–response curves. Intact endothelium was confirmed when rings relaxed >80% in response to acetylcholine but the absence was considered when response was <10%. Data were expressed as percentage of vascular relaxation relative to maximal contraction induced by phenylephrine. Fifty percentage of the concentration to induce vascular relaxation was determined for LASSBio-1860 (EC_{50}) in the absence and presence of previous exposure (30 min) to pharmacological antagonists of adenosine A_2A and A_2B receptors, ZM-241385 (3 μM) and MRS-1706 (1 μM), respectively. To investigate the involvement of PDE and cAMP formation pathway, rings were preincubated for 30 minutes with LASSBio-1860 (1 μM) followed by exposure to cumulative concentration of isoproterenol (10^{-9} to 10^{-6} M).

4.4. PAH Induction

PAH was induced in male Wistar rats (200-250 g) by a single intraperitoneal injection of monocrotaline (MCT, 60 mg/kg). Two weeks after PAH induction, the increase in mPAP was confirmed using transthoracic echocardiography, based on the increase of pulmonary artery acceleration time and total ejection time ratio (PAAT/TET). After confirmation, animals were randomly divided into five experimental groups: (1) control, (2) PAH + vehicle, (3) PAH + LASSBio-1860 (62 mg/kg/day p.o.), (4) PAH + hMSC (10^5 cells) and (5) PAH + LASSBio-1860 + hMSC. A single dose of 10^5 hMSC was intravenously administered into the caudal vein followed by 14 days of oral treatment with LASSBio-1860. Vehicle groups received the same volume (300 μL) of DNase I in PBS

 doi:10.20944/preprints202512.0045.v1

(0.6 U/mL). Umbilical cord–derived hMSCs were isolated and immunophenotyped following Alencar et al. [45].

4.5. Transthoracic Echocardiography

Transthoracic echocardiography was performed under anesthesia with isoflurane 1.5% using a ultrasound system (Philips CX50 Healthcare, Andover, MA, USA) coupled to a 12-4 MHz probe. Animals were placed in the supine position on a heated platform, and heart rate was monitored throughout the procedure. Parasternal long-axis and short-axis images were obtained, along with pulmonary artery doppler measurements to determine PAAT/TET and confirm PAH. After 14 days of treatment, echocardiography was repeated to obtain the following hemodynamic parameters: PAAT/TET, cardiac output and RV anterior wall thickness. Parameters of left-ventricular structure and function were obtained to exclude left-sided heart failure and post-capillary pulmonary hypertension.

4.6. Cardiac Catheterism

Animals were anesthetized with ketamine (80 mg/kg) and xylazine (15 mg/kg), and right ventricular pressure was directly measured by ventricular puncture using a needle, through toracotomy, connected to a pressure transducer interfaced with Lab Chart software (Version 7.0, ADInstruments, Inc.).

4.7. Morphometric and Histological Analysis

At the end of experimental protocol, animals were euthanized, and tissues were weighed and prepared for histological and protein expression analyses. The ratio of RV and left ventricle plus septum weight (RV/LV+S) was calculated to assess RV hypertrophy (Fulton index). Cardiac tissues were stored at −80 °C for subsequent protein expression analyse, while pulmonary tissue was fixed in a 10% formaldehyde solution and embedded in paraffin for histological evaluation. Paraffin-embedded samples were sectioned at 5 μm using a microtome (Lupe, MRP-03) and inflammatory infiltrates were assessed on hematoxylin–eosin–stained sections. Cells were counted at 400× within one vessel diameter of the external elastic lamina (cells·HPF^{-1}). Interstitial cells were examined in ten fields per slide with a digital camera (Canon, USA) coupled to a light microscope at 400× magnification (Axiostar plus, Zeiss, Germany). Using the same histological staining and method, the vessel wall thickness was obtained calculating the percentage of vessel diameter over the total external area.

4.8. Membrane Preparation and Western Blot

Heart samples were rapidly excised and frozen in liquid nitrogen. For protein extraction, tissues were kept on ice and mechanically homogenized with lysis buffer (12.5% sucrose, 20 mM Tris-HCl, pH 7.4, 1 mM EDTA) supplemented with protease inhibitors (1 mM phenylmethylsulfonyl fluoride, 1 mM benzamidine, 1 mM dithiothreitol, 1 μg/mL pepstatin A, 1 μg/mL chymostatin, 1 μg/mL aprotinin, 1 μg/mL leupeptin, and 1 μg/mL antipain). Homogenates were clarified by centrifugation (5 min, 1,000 × g, 4 °C); supernatants were collected and stored at −80 °C. Protein concentration was determined by the Coomassie (Bradford) method using bovine serum albumin standards. Aliquots were mixed 1:1 with 2× Laemmli sample buffer containing 5% β-mercaptoethanol, heated for 5 min at 95 °C, and equal amounts of total protein (50 μg per lane) were resolved on 10% SDS–polyacrylamide gels. Proteins were transferred to nitrocellulose membranes using a semi-dry apparatus (Bio-Rad, Hercules, CA, USA). Transfer quality and equal loading were verified by Ponceau S staining. Membranes were blocked for 1 h at room temperature in PBS containing 5% non-fat dry milk and 0.1% Tween-20 (PBS-T), then incubated overnight at 4 °C with primary antibodies diluted in PBS-T: TGF-β (1:1000), CAMKII (1:1000), and anti-GAPDH (1:1000). After three washes in PBS-T (5 min each), membranes were incubated for 1 h at room temperature with HRP-conjugated

 doi:10.20944/preprints202512.0045.v1

secondary antibodies (1:10,000 in PBS-T), washed again, and developed by enhanced chemiluminescence. Chemiluminescent detection of specific bands were captured on an ImageQuant LAS-4000 system (GE Healthcare, Chicago, IL, USA).

4.9. Statistical Analysis

Data are expressed as the mean ± SEM. The one-way ANOVA followed by Tukey's post hoc test was used for comparison (GraphPad Prism, version 6, San Diego, CA, USA). Differences between the experimental groups were considered statistically significant at $p < 0.05$.

5. Conclusion

Combination of LASSBio-1860 and hMSCs improved ventricular function; reduced vascular and right-ventricular remodeling; and decreased inflamattory and proliferative changes induced by MCT-induced PAH (Figure 9).

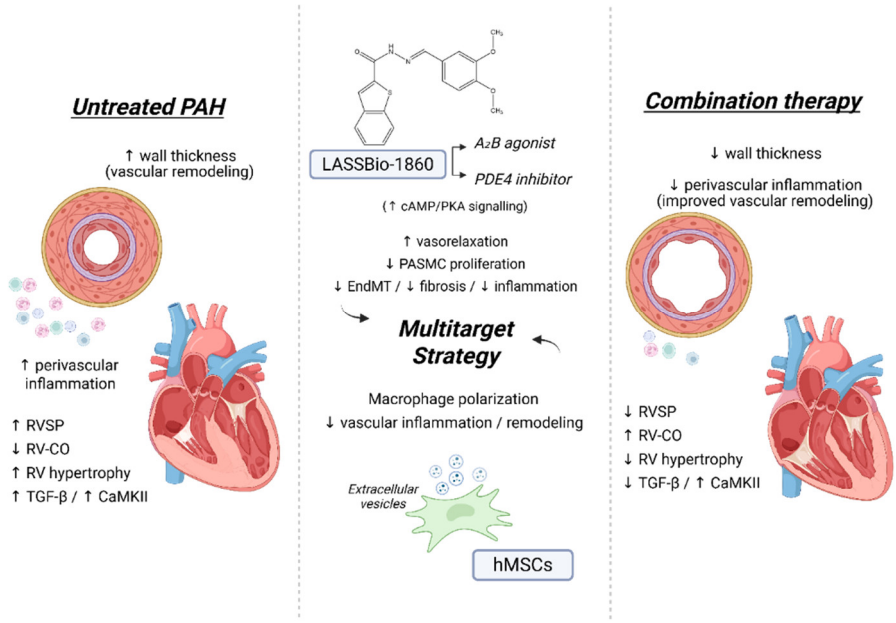

Figure 9. Multitarget combination of LASSBio-1860 and hMSCs in monocrotaline-induced PAH. LASSBio-1860, a dual A_2B adenosine receptor agonist and PDE4 inhibitor, enhances cAMP/PKA signalling and exerts vasorelation and anti-remodeling effects, while hMSCs and their extracellular vesicles provide complementary paracrine immunomodulation. Together, these actions reduce pulmonary vascular remodeling, perivascular inflammation, RVSP and RV hypertrophy, restore RV cardiac output and downregulate TGF-β and CaMKII.

Author Contributions: Conceptualization, T.L.M., G.Z.-S.; Methodology, B.E.D., J.F.V., R.C.M.; Validation, B.E.D., A.J.S.J, T.L.M., R.C.M.; Formal analysis, B.E.D., R.M.O.; Investigation, B.E.D., L.S.F., A.J.S.J.; Resources, T.L.M., G.Z.-S.; Writing—original draft preparation, B.E.D.; Writing—review and editing, T.L.M., R.M.O., G.Z.-S.; Visualization, T.L.M., B.E.D; P.S.M.P; Supervision, G.Z.-S.; R.M.O. Project administration, G.Z.-S.; R.M.O. Funding acquisition, G.Z.-S. All authors have read and agreed to the published version of the manuscript.

Funding: This research was funded by Fundação Carlos Chagas Filho de Amparo a Pesquisa do Estado do Rio de Janeiro - FAPERJ, grant number E-26/200.881/2021.

Institutional Review Board Statement: The animal study protocol was approved by the Ethics Committee of Federal University of Rio de Janeiro (protocol code 018/23, date of approval: 07/11/2023).

Data Availability Statement: Not applicable.

Conflicts of Interest: The authors declare no conflict of interest.

 doi:10.20944/preprints202512.0045.v1

References

1. Bousseau, S.; Sobrano Fais, R.; Gu, S.; Frump, A.; Lahm, T. Pathophysiology and New Advances in Pulmonary Hypertension. BMJ Med. 2023, 2, e000137, doi:10.1136/bmjmed-2022-000137.
2. Simonneau, G.; Montani, D.; Celermajer, D.S.; Denton, C.P.; Gatzoulis, M.A.; Krowka, M.; Williams, P.G.; Souza, R. Haemodynamic Definitions and Updated Clinical Classification of Pulmonary Hypertension. Eur. Respir. J. 2019, 53, doi:10.1183/13993003.01913-2018.
3. Benza, R.L.; Miller, D.P.; Barst, R.J.; Badesch, D.B.; Frost, A.E.; McGoon, M.D. An Evaluation of Long-Term Survival from Time of Diagnosis in Pulmonary Arterial Hypertension from the Reveal Registry. Chest 2012, 142, 448–456, doi:10.1378/chest.11-1460.
4. Galiè, N.; Barberà, J.A.; Frost, A.E.; Ghofrani, H.-A.; Hoeper, M.M.; McLaughlin, V.V.; Peacock, A.J.; Simonneau, G.; Vachiery, J.-L.; Grünig, E.; et al. Initial Use of Ambrisentan plus Tadalafil in Pulmonary Arterial Hypertension. N. Engl. J. Med. 2015, 373, 834–844, doi:10.1056/NEJMoa1413687.
5. Peacock, A.J.; Zamboni, W.; Vizza, C.D. Ambrisentan for the Treatment of Adults with Pulmonary Arterial Hypertension: A Review. Curr. Med. Res. Opin. 2015, 31, 1793–1807, doi:10.1185/03007995.2015.1074890.
6. Makowski, C.T.; Rissmiller, R.W.; Bullington, W.M. Riociguat: A Novel New Drug for Treatment of Pulmonary Hypertension. Pharmacotherapy 2015, 35, 502–519, doi:10.1002/phar.1592.
7. Ausó, E.; Gómez-Vicente, V.; Esquiva, G. Visual Side Effects Linked to Sildenafil Consumption: An Update. Biomedicines 2021, 9, 291, doi:10.3390/biomedicines9030291.
8. Frantz, R.P.; Hill, J.W.; Lickert, C.A.; Wade, R.L.; Cole, M.R.; Tsang, Y.; Drake, W. Medication Adherence, Hospitalization, and Healthcare Resource Utilization and Costs in Patients with Pulmonary Arterial Hypertension Treated with Endothelin Receptor Antagonists or Phosphodiesterase Type-5 Inhibitors. Pulm. Circ. 2020, 10, 2045894019880086, doi:10.1177/2045894019880086.
9. Evans, C.E.; Cober, N.D.; Dai, Z.; Stewart, D.J.; Zhao, Y.-Y. Endothelial Cells in the Pathogenesis of Pulmonary Arterial Hypertension. Eur. Respir. J. 2021, 58, 2003957, doi:10.1183/13993003.03957-2020.
10. Gallardo-Vara, E.; Ntokou, A.; Dave, J.M.; Jovin, D.G.; Saddouk, F.Z.; Greif, D.M. Vascular Pathobiology of Pulmonary Hypertension. J. Heart Lung Transplant. Off. Publ. Int. Soc. Heart Transplant. 2023, 42, 544–552, doi:10.1016/j.healun.2022.12.012.
11. Stacher, E.; Graham, B.B.; Hunt, J.M.; Gandjeva, A.; Groshong, S.D.; McLaughlin, V.V.; Jessup, M.; Grizzle, W.E.; Aldred, M.A.; Cool, C.D.; et al. Modern Age Pathology of Pulmonary Arterial Hypertension. Am. J. Respir. Crit. Care Med. 2012, 186, 261–272, doi:10.1164/rccm.201201-0164OC.
12. Waszak, P.; Alphonse, R.; Vadivel, A.; Ionescu, L.; Eaton, F.; Thébaud, B. Preconditioning Enhances the Paracrine Effect of Mesenchymal Stem Cells in Preventing Oxygen-Induced Neonatal Lung Injury in Rats. Stem Cells Dev. 2012, 21, 2789–2797, doi:10.1089/scd.2010.0566.
13. Xu, J.-H.; Liang, J.-P.; Zhu, C.-J.; Lian, Y.-J. Mesenchymal Stem Cell-Derived Extracellular Vesicles Therapy for Pulmonary Hypertension: A Comprehensive Review of Preclinical Studies. J. Intervent. Cardiol. 2022, 2022, 5451947, doi:10.1155/2022/5451947.
14. Loisel, F.; Provost, B.; Haddad, F.; Guihaire, J.; Amsallem, M.; Vrtovec, B.; Fadel, E.; Uzan, G.; Mercier, O. Stem Cell Therapy Targeting the Right Ventricle in Pulmonary Arterial Hypertension: Is It a Potential Avenue of Therapy? Pulm. Circ. 2018, 8, 2045893218755979, doi:10.1177/2045893218755979.
15. Gorelova, A.; Berman, M.; Al Ghouleh, I. Endothelial-to-Mesenchymal Transition in Pulmonary Arterial Hypertension. Antioxid. Redox Signal. 2021, 34, 891–914, doi:10.1089/ars.2020.8169.
16. Shah, A.J.; Beckmann, T.; Vorla, M.; Kalra, D.K. New Drugs and Therapies in Pulmonary Arterial Hypertension. Int. J. Mol. Sci. 2023, 24, 5850, doi:10.3390/ijms24065850.
17. Boucherat, O.; Bonnet, S.; Provencher, S.; Potus, F. Anti-Remodeling Therapies in Pulmonary Arterial Hypertension. Trends Pharmacol. Sci. 2025, 46, 674–691, doi:10.1016/j.tips.2025.05.004.
18. Beltrame, F.; Nascimento-Carlos, B.; da Silva, J.S.; Maia, R.C.; Montagnoli, T.L.; Barreiro, E.J.; Zapata-Sudo, G. Novel Agonists of Adenosine Receptors in Animal Model of Acute Myocardial Infarction. Drug Des. Devel. Ther. 2024, 18, 5211–5223, doi:10.2147/DDDT.S464712.
19. Rocha, M.D.D. Novos protótipos heteroaril-n-acilidrazônicos multialvos planejados para o tratamento da hipertensão arterial pulmonar, UFRJ: Rio de Janeiro, 2017.

20. Alencar, A.K.N.; Montes, G.C.; Barreiro, E.J.; Sudo, R.T.; Zapata-Sudo, G. Adenosine Receptors As Drug Targets for Treatment of Pulmonary Arterial Hypertension. Front. Pharmacol. 2017, 8, doi:10.3389/fphar.2017.00858.
21. Dubey, R.K.; Baruscotti, I.; Stiller, R.; Fingerle, J.; Gillespie, D.G.; Mi, Z.; Leeners, B.; Imthurn, B.; Rosselli, M.; Jackson, E.K. Adenosine, Via A2B Receptors, Inhibits Human (P-SMC) Progenitor Smooth Muscle Cell Growth. Hypertension 2020, 75, 109–118, doi:10.1161/HYPERTENSIONAHA.119.13698.
22. Qian, G.; Cao, J.; Chen, C.; Wang, L.; Huang, X.; Ding, C.; Cai, X.; Yin, F.; Chu, J.; Li, G.; et al. Paeoniflorin Inhibits Pulmonary Artery Smooth Muscle Cells Proliferation via Upregulating A2B Adenosine Receptor in Rat. PLOS ONE 2013, 8, e69141, doi:10.1371/journal.pone.0069141.
23. Eckly-Michel, A.; Martin, V.; Lugnier, C. Involvement of Cyclic Nucleotide-Dependent Protein Kinases in Cyclic AMP-Mediated Vasorelaxation. Br. J. Pharmacol. 1997, 122, 158–164, doi:10.1038/sj.bjp.0701339.
24. Xing, Y.; Hou, Y.; Fan, T.; Gao, R.; Feng, X.; Li, B.; Pang, J.; Guo, W.; Shu, T.; Li, J.; et al. Endothelial Phosphodiesterase 4B Inactivation Ameliorates Endothelial-to-Mesenchymal Transition and Pulmonary Hypertension. Acta Pharm. Sin. B 2024, 14, 1726–1741, doi:10.1016/j.apsb.2024.01.012.
25. Jin, S.-L.C.; Ding, S.-L.; Lin, S.-C. Phosphodiesterase 4 and Its Inhibitors in Inflammatory Diseases. Chang Gung Med. J. 2012, 35, 197–210, doi:10.4103/2319-4170.106152.
26. Fan, T.; Wang, W.; Wang, Y.; Zeng, M.; Liu, Y.; Zhu, S.; Yang, L. PDE4 Inhibitors: Potential Protective Effects in Inflammation and Vascular Diseases. Front. Pharmacol. 2024, 15, 1407871, doi:10.3389/fphar.2024.1407871.
27. da Silva, M. de M.C.; de Alencar, A.K.N.; da Silva, J.S.; Montagnoli, T.L.; da Silva, G.F.; Rocha, B. de S.; Montes, G.C.; Mendez-Otero, R.; Pimentel-Coelho, P.M.; Vasques, J.F.; et al. Therapeutic Benefit of the Association of Lodenafil with Mesenchymal Stem Cells on Hypoxia-Induced Pulmonary Hypertension in Rats. Cells 2020, 9, 2120, doi:10.3390/cells9092120.
28. Luo, Q.; Wang, X.; Liu, R.; Qiao, H.; Wang, P.; Jiang, C.; Zhang, Q.; Cao, Y.; Yu, H.; Qu, L. alpha1A-Adrenoceptor Is Involved in Norepinephrine-Induced Proliferation of Pulmonary Artery Smooth Muscle Cells via CaMKII Signaling. J. Cell. Biochem. 2019, 120, 9345–9355, doi:10.1002/jcb.28210.
29. Anderson, M.E.; Brown, J.H.; Bers, D.M. CaMKII in Myocardial Hypertrophy and Heart Failure. J. Mol. Cell. Cardiol. 2011, 51, 468–473, doi:10.1016/j.yjmcc.2011.01.012.
30. Chen, Y.; Liu, J.; Zhang, Q.; Chai, L.; Chen, H.; Li, D.; Wang, Y.; Qiu, Y.; Shen, N.; Zhang, J.; et al. Activation of CaMKII/HDAC4 by SDF1 Contributes to Pulmonary Arterial Hypertension via Stabilization Runx2. Eur. J. Pharmacol. 2024, 970, 176483, doi:10.1016/j.ejphar.2024.176483.
31. Wójcik-Pszczoła, K.; Chłoń-Rzepa, G.; Jankowska, A.; Ślusarczyk, M.; Ferdek, P.E.; Kusiak, A.A.; Świerczek, A.; Pociecha, K.; Koczurkiewicz-Adamczyk, P.; Wyska, E.; et al. A Novel, Pan-PDE Inhibitor Exerts Anti-Fibrotic Effects in Human Lung Fibroblasts via Inhibition of TGF-β Signaling and Activation of cAMP/PKA Signaling. Int. J. Mol. Sci. 2020, 21, 4008, doi:10.3390/ijms21114008.
32. Cai, Z.; Tu, L.; Guignabert, C.; Merkus, D.; Zhou, Z. Purinergic Dysfunction in Pulmonary Arterial Hypertension. J. Am. Heart Assoc. 2020, 9, e017404, doi:10.1161/JAHA.120.017404.
33. Mertens, T.C.J.; Hanmandlu, A.; Tu, L.; Phan, C.; Collum, S.D.; Chen, N.-Y.; Weng, T.; Davies, J.; Liu, C.; Eltzschig, H.K.; et al. Switching-Off Adora2b in Vascular Smooth Muscle Cells Halts the Development of Pulmonary Hypertension. Front. Physiol. 2018, 9, 555, doi:10.3389/fphys.2018.00555.
34. Karmouty-Quintana, H.; Philip, K.; Acero, L.F.; Chen, N.-Y.; Weng, T.; Molina, J.G.; Luo, F.; Davies, J.; Le, N.-B.; Bunge, I.; et al. Deletion of ADORA2B from Myeloid Cells Dampens Lung Fibrosis and Pulmonary Hypertension. FASEB J. Off. Publ. Fed. Am. Soc. Exp. Biol. 2015, 29, 50–60, doi:10.1096/fj.14-260182.
35. Puertas-Umbert, L.; Alonso, J.; Hove-Madsen, L.; Martínez-González, J.; Rodríguez, C. PDE4 Phosphodiesterases in Cardiovascular Diseases: Key Pathophysiological Players and Potential Therapeutic Targets. Int. J. Mol. Sci. 2023, 24, 17017, doi:10.3390/ijms242317017.
36. Beca, S.; Helli, P.B.; Simpson, J.A.; Zhao, D.; Farman, G.P.; Jones, P.; Tian, X.; Wilson, L.S.; Ahmad, F.; Chen, S.R.W.; et al. Phosphodiesterase 4D Regulates Baseline Sarcoplasmic Reticulum Ca2+ Release and Cardiac Contractility, Independently of L-Type Ca2+ Current. Circ. Res. 2011, 109, 1024–1030, doi:10.1161/CIRCRESAHA.111.250464.

37. Growcott, E.J.; Spink, K.G.; Ren, X.; Afzal, S.; Banner, K.H.; Wharton, J. Phosphodiesterase Type 4 Expression and Anti-Proliferative Effects in Human Pulmonary Artery Smooth Muscle Cells. Respir. Res. 2006, 7, 9, doi:10.1186/1465-9921-7-9.
38. Zhang, Q.; Liu, H.; Liu, C.; Wang, Y.; Huang, P.; Wang, X.; Ma, Y.; Ma, L.; Ge, R. Tibetan Mesenchymal Stem Cell-Derived Exosomes Alleviate Pulmonary Vascular Remodeling in Hypoxic Pulmonary Hypertension Rats. Stem Cells Dayt. Ohio 2024, 42, 720–735, doi:10.1093/stmcls/sxae032.
39. Hu, L.; Wang, J.; Lin, D.; Shen, Y.; Huang, H.; Cao, Y.; Li, Y.; Li, K.; Yu, Y.; Yu, Y.; et al. Mesenchymal Stem Cell-Derived Nanovesicles as a Credible Agent for Therapy of Pulmonary Hypertension. Am. J. Respir. Cell Mol. Biol. 2022, 67, 61–75, doi:10.1165/rcmb.2021-0415OC.
40. Xu, J.-H.; Liang, J.-P.; Zhu, C.-J.; Lian, Y.-J. Mesenchymal Stem Cell-Derived Extracellular Vesicles Therapy for Pulmonary Hypertension: A Comprehensive Review of Preclinical Studies. J. Intervent. Cardiol. 2022, 2022, 5451947, doi:10.1155/2022/5451947.
41. Santos, R.T.; Braga, C.L.; de Sá Freire Onofre, M.E.; da Silva, C.M.; de Novaes Rocha, N.; Veras, R.G.; de Souza Serra, S.S.; Teixeira, D.E.; dos Santos Alves, S.A.; Miranda, B.T.; et al. Cardioprotective Effects of Extracellular Vesicles from Hypoxia-Preconditioned Mesenchymal Stromal Cells in Experimental Pulmonary Arterial Hypertension. Stem Cell Res. Ther. 2025, 16, 466, doi:10.1186/s13287-025-04604-y.
42. Klinger, J.R.; Pereira, M.; Del Tatto, M.; Brodsky, A.S.; Wu, K.Q.; Dooner, M.S.; Borgovan, T.; Wen, S.; Goldberg, L.R.; Aliotta, J.M.; et al. Mesenchymal Stem Cell Extracellular Vesicles Reverse Sugen/Hypoxia Pulmonary Hypertension in Rats. Am. J. Respir. Cell Mol. Biol. 2020, 62, 577–587, doi:10.1165/rcmb.2019-0154OC.
43. Wan, M.; Lu, C.; Liu, Y.; Luo, F.; Zhou, J.; Xu, F. Mesenchymal Stem Cell-Derived Extracellular Vesicles Prevent the Formation of Pulmonary Arterial Hypertension through a microRNA-200b-Dependent Mechanism. Respir. Res. 2023, 24, 233, doi:10.1186/s12931-023-02474-7.
44. Hansmann, G.; Chouvarine, P.; Diekmann, F.; Giera, M.; Ralser, M.; Mülleder, M.; von Kaisenberg, C.; Bertram, H.; Legchenko, E.; Hass, R. Human Umbilical Cord Mesenchymal Stem Cell-Derived Treatment of Severe Pulmonary Arterial Hypertension. Nat. Cardiovasc. Res. 2022, 1, 568–576, doi:10.1038/s44161-022-00083-z.
45. Alencar, A.K.N.; Pimentel-Coelho, P.M.; Montes, G.C.; da Silva, M. de M.C.; Mendes, L.V.P.; Montagnoli, T.L.; Silva, A.M.S.; Vasques, J.F.; Rosado-de-Castro, P.H.; Gutfilen, B.; et al. Human Mesenchymal Stem Cell Therapy Reverses Su5416/Hypoxia-Induced Pulmonary Arterial Hypertension in Mice. Front. Pharmacol. 2018, 9, 1395, doi:10.3389/fphar.2018.01395.
46. Oh, S.; Jung, J.-H.; Ahn, K.-J.; Jang, A.Y.; Byun, K.; Yang, P.C.; Chung, W.-J. Stem Cell and Exosome Therapy in Pulmonary Hypertension. Korean Circ. J. 2022, 52, 110–122, doi:10.4070/kcj.2021.0191.
47. Humbert, M.; McLaughlin, V.V.; Badesch, D.B.; Ghofrani, H.A.; Gibbs, J.S.R.; Gomberg-Maitland, M.; Preston, I.R.; Souza, R.; Waxman, A.B.; Moles, V.M.; et al. Sotatercept in Patients with Pulmonary Arterial Hypertension at High Risk for Death. N. Engl. J. Med. 2025, 392, 1987–2000, doi:10.1056/NEJMoa2415160.
48. Gewehr, D.M.; Salgueiro, G.R.; Noronha, L. de; Kubrusly, F.B.; Kubrusly, L.F.; Coltro, G.A.; Preto, P.C.; Bertoldi, A. de S.; Vieira, H.I. Plexiform Lesions in an Experimental Model of Monocrotalin-Induced Pulmonary Arterial Hypertension. Arq. Bras. Cardiol. 2020, 115, 480–490, doi:10.36660/abc.20190306.
49. Urboniene, D.; Haber, I.; Fang, Y.-H.; Thenappan, T.; Archer, S.L. Validation of High-Resolution Echocardiography and Magnetic Resonance Imaging vs. High-Fidelity Catheterization in Experimental Pulmonary Hypertension. Am. J. Physiol. - Lung Cell. Mol. Physiol. 2010, 299, L401–L412, doi:10.1152/ajplung.00114.2010.